Series Solution For a Peristaltic Flow of a Magneto-fluid Through a Taper Eccentric Cylinders

Kh Mekheimer, M Mohamed and Shurouq Alnufiai

Abstract— In this paper the magneto-hydrodynamic peristaltic flow of an incompressible Newtonian fluid was investigated between two eccentric tubes. The problem is measured in cylindrical coordinates. Geometrically, we considered two eccentric tubes in which the inner tube is rigid while the outer tube is tapered and have a sinusoidal wave generated on its walls. The governing equations are observed nonlinear second order partial differential equations under the conditions of long wavelength approximation. The problem has been solved with the help of the homotopy perturbation method. The obtained results are then plotted to see the influence of the different physical parameters on the velocity, pressure gradient and pressure rise expressions. The velocity profile is drawn in the two and three dimensions. The trapping boluses are also discussed through the contour plot of the streamlines.

Index Terms— Peristaltic flow; Taper Eccentric Cylinders; series solution method; Magneto-fluid.

1 Introduction

Peristalsis pumping is a phenomenon in which fluid transport happens when a gradual wave of area contraction or expansion propagates along the length of distensible duct. Peristalsis is one of the topic highly important in applied mathematics, engineering, physiological world and its have many applications in real life. It is an automatic and vital process that moves food through the digestive tract, transport urine from kidney to bladder, in the vasomotion of small blood vessels such as venues, capillaries and arterioles. And also the mechanism of peristaltic transport has been exploited for industrial applications like sanitary fluid transport, corrosive fluids, a toxic liquid transport in the nuclear industry. The peristaltic transport with long wavelength at low Reynolds number [1,2] with all Reynold numbers [3] or for long and short wavelength [4] have been analyzed. RACHID, [5] studied The effect of a pulsatile flow on the Peristaltic Output: Case of a Newtonian Fluid. Moreover, with through a porous medium by Afifi NAS et al. [6]. Mekheimer [7] has shown the effect of the induced magnetic field on the peristaltic flow of a couple stress fluid. Ellahi, et al [8]. Studied Series Solutions of Magnetohydrodynamic peristaltic flow of a jeffrey fluid in eccentric cylinders. The magnetic field effects of different types of fluids [8-10]. A lot of investigations are available in the literature to study the effect of an endoscope on peristaltic motion of Newtonian and non-Newtonian fluids [11-13]. Mekheimer [14] studied The micropolar fluid model for blood flow through a tapered artery with a stenosis Also with Peristaltic Transport in channel [15,16]. Misra and Pandey [17] studied peristaltic transport in a tapered tube. In the present work we discuss the peristaltic flow of newtonian fluids under the effect of the magnetic field in an eccentric cylinder. Which the inner tube is rigid while the outer have a sinusoidal wave generated on its tapered walls. Peristaltic pumping characteristics are discussed in detail. The flow analysis is developed in the unsteady state by using the long wavelength approximation. The problem is first modeled and then solved an alyticall for the axial velocity, axial pressure gradient and pressure rise. This analysis gives a better judgement for the speed of injection and the fluid flow characteristics in the syringe. Also, the injection can be carried out more proficiently and pain of the patient can be extenuated.

- *Kh S Mekherimer prof of Applied Mathematics ,Egypt E-mail:S_Math223 @mail.com*
- ***Shurouq Alnufiai*** *is currently have masters degree in* Bio-Fluid mechanics, *Saudi Arabia ,E-mail: marth.89@mail.com*

2 Mathematical Formulation Of The Problem:

Consider a MHD flow of an incompressible Newtonian fluid through eccentric tubes. The inner tube is rigid (endoscope or catheter) and the outer have a sinusoidal wave generated on the walls of tapered. The radius of the inner tube is δ' but we need to reference the fluid motion to the center of the outer tube. The center of the inner tube is now at position $z' = \varepsilon', y' = 0$ where and are coordinates in the cross-section of the pipe as shown in figure 3.1 Then the boundary of the inner tube is described to order ε' by $r_1' = \delta' + \varepsilon' \cos[\theta']$. (obtained by using the cosine rule) where $(\varepsilon' << \delta')$ is the parameter that controls the eccentricity of the inner tube position. The geometry of the walls surface is described in fig.(1).

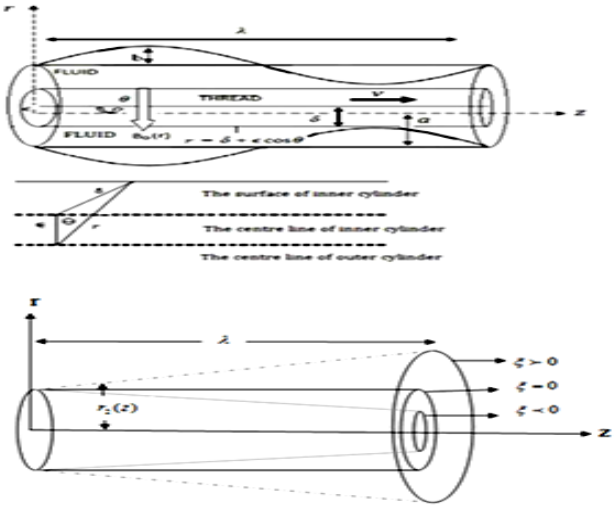

Fig 1 The simplified model of geometry of the problem

The equations for the radii are

$$r_1' = \delta' + \varepsilon' \cos[\theta'],$$
$$r_2' = a_1'(z') + b\cos[\frac{2\pi}{\lambda}(z' - ct')],$$
$$a_1'(z) = a + + z'\xi'(z') \quad (1)$$

Where $a_1'(z)$ is the radius of the tapered tube segment in the annulus region, a is the radius of outer tube at the non-tapered wall , ξ is the tapering parameter, δ' is the radius of the inner tube, b is the amplitude of the wave, λ is the wavelength, c is the propagation velocity and t' is the time. The problem has been studied in a cylindrical coordinate system (r', θ', z') radial, azimuthal and axial coordinates respectively.

The equations of motion of the flow in the gap between the inner and the outer tubes are

$$\frac{\partial u'}{\partial z'} + \frac{\partial v'}{\partial r'} + \frac{v'}{r'} + \frac{1}{r'}\frac{\partial w'}{\partial \theta'} = 0 \quad (2)$$

$$\rho[\frac{\partial u'}{\partial t'} + u'\frac{\partial u'}{\partial z'} + v'\frac{\partial u'}{\partial r'} + \frac{w'}{r'}\frac{\partial u'}{\partial \theta'}] = -\frac{\partial p'}{\partial z'} + \mu[\frac{\partial^2 u'}{\partial z'^2} + \frac{\partial^2 u'}{\partial r'^2} + \frac{1}{r'}\frac{\partial u'}{\partial r'} + \frac{1}{r'^2}\frac{\partial^2 u'}{\partial \theta'^2}] - \frac{\sigma a^2 B_0^2(r)}{\rho}u' \quad (3)$$

$$\rho[\frac{\partial v'}{\partial t'} + u'\frac{\partial v'}{\partial z'} + v'\frac{\partial v'}{\partial r'} + \frac{w'}{r'}\frac{\partial v'}{\partial \theta'} - \frac{w'^2}{r'}] = -\frac{\partial p'}{\partial r'} + \mu[\frac{\partial^2 v'}{\partial z'^2} + \frac{\partial^2 v'}{\partial r'^2} + \frac{1}{r'}\frac{\partial v'}{\partial r'} + \frac{1}{r'^2}\frac{\partial^2 v'}{\partial \theta'^2} - \frac{v'}{r'^2} - \frac{2}{r'^2}\frac{\partial^2 w'}{\partial \theta'^2}] \quad (4)$$

$$\rho[\frac{\partial w'}{\partial t'} + u'\frac{\partial w'}{\partial z'} + v'\frac{\partial w'}{\partial r'} + \frac{w'}{r'}\frac{\partial w'}{\partial \theta'} + \frac{w'v'}{r'}] = -\frac{\partial p'}{\partial \theta'} + \mu[\frac{\partial^2 w'}{\partial z'^2} + \frac{\partial^2 w'}{\partial r'^2} + \frac{1}{r'}\frac{\partial w'}{\partial r'} + \frac{1}{r'^2}\frac{\partial^2 w'}{\partial \theta'^2} - \frac{w'}{r'^2} + \frac{2}{r'^2}\frac{\partial v'}{\partial \theta'}] \quad (5)$$

Where v', w', u' are the velocity components in r', θ' and z'- directions, respectively, ρ is the density, p' is the pressure and μ is the viscosity, $B_0(r)$ is the magnetic field, σ is the electrical conductivity.

The boundary conditions are:

$$u' = 0 \quad at \quad r' = r'$$
$$u' = V' \quad at \quad r' = r_1' \quad (6)$$

It is convenient to non-dimensionalize the variables appearing in equations (2-5) and introducing Reynolds number Re, wave number ratio δ as follows: (7)

$$p = \frac{a^2}{\mu c\lambda}p', u = \frac{u'}{c}, v = \frac{v'}{c}, w = \frac{w'}{c}, \theta = \theta', t = \frac{c}{\lambda}t', Re = \frac{\rho ca}{\mu}, r_1 = \frac{r_1'}{a} = \frac{\delta'}{a} + \frac{\varepsilon'}{a}cos(\theta')$$
$$\varphi^* = \frac{b}{a}, \ \delta = \frac{\delta'}{a}, \ \varepsilon = \frac{\varepsilon'}{a}, \ \delta_0 = \frac{a}{\lambda}, \ z = \frac{z'}{\lambda}, \ r_2 = \frac{r_2'}{a} = 1 + \frac{\lambda\xi z}{a} + \frac{b}{a}cos(2\pi os - t)),$$
$$\overline{M}^2(r) = \frac{\sigma B_0^2(r)a^2}{\mu}, \xi = \xi'$$

Where Re is the Reynolds number, M is the Hartmann number, the parameter of taper is($\xi = \tan\phi$)[14], ϕ is called the taper angle and for the converging tapering ($\xi < 0$), non-tapered artery ($\xi = 0$) and the diverging tapering ($\xi > 0$) as shown in (Fig.1) . δ_0 is the dimensionless wave ber and ε is eccentricity parameter. ϕ^* is the amplitude ratio. After using the above assumption and the long velength approimation ($\delta_0 \to 0$) then taking the $\overline{M} = \frac{M}{r}$ equ uations of motion in the dimensionless form become:

$$\frac{\partial u}{\partial z} = 0, \quad (8)$$

$$\frac{\partial p}{\partial z} = \left[\delta_0^2\frac{\partial^2 u}{\partial z^2} + \frac{\partial^2 u}{\partial r^2} + \frac{1}{r}\frac{\partial u}{\partial r} + \frac{1}{r^2}\frac{\partial^2 u}{\partial \theta^2}\right] - \frac{M^2}{r^2}u \quad (9)$$

$$\frac{\partial p}{\partial r} = 0, \quad (10)$$

$$\frac{\partial p}{\partial \theta} = 0 \quad (11)$$

Eqs. (10, 11) shows that p is not a function of r and θ. The corresponding boundary conditions in non-dimensional form are

$$u = 0, \quad \text{at} \quad r = r_2 = 1 + \frac{\lambda\xi z}{a} + \phi^*\cos[2\pi(z - t)], \quad (12)$$
$$u = V, \quad \text{at} \quad r = r_1 = \delta + \varepsilon\cos[\theta] \quad (13)$$

3 Solution Of The Problem

Solution of the above boundary value problem is obtained by the series solution method [18]. The deformation equation for the given problem is defined as

$$H(u, f) = (1 - f)(\ell[\tilde{u}] - \ell[\tilde{u}_0]) + f(\ell[\tilde{u}] + \frac{1}{r^2}\frac{\partial^2\tilde{u}}{\partial\theta^2} - \frac{dp}{dz}) = 0 \quad (14)$$

where ℓ, the linear operator is assumed to be $\ell = \frac{\partial^2}{\partial r^2} + \frac{1}{r}\frac{\partial}{\partial r} - \frac{M}{r}$

We define the following initial guess satisfying the boundary conditions

$$\tilde{u}_0 = V\ Sinh(M(Log[\frac{r}{r_2}]))\ Csch[M(Log[\frac{r_1}{r_2}])], \quad (15)$$

Now we describe

$$\tilde{u}(r,\theta,z,t,f) = u_0 + f u_1 + f^2 u_2 + \ldots \tag{16}$$

Using the above equation into Eq. (14) and then finding the terms of the first two orders of embedding parameter f, we get the following problems including boundary conditions

Zeroth order system:

$$\ell[u_0] - \ell[\tilde{u}_0] = 0 \tag{17}$$

$$u_0 = 0, \text{ at } r = r_2 \tag{18}$$

$$u_0 = V, \text{ at } r = r_1 \tag{19}$$

The solution of the above zeroth order system can be obtained by using Eq. (15) and is simply found as

$$u_0(r,\theta,z,t,f) = \tilde{u}_0 = V \,\mathrm{Sinh}(M(\mathrm{Log}[\frac{r}{r_2}]))\,\mathrm{Csch}[M(\mathrm{Log}[\frac{r_1}{r_2}])] \tag{20}$$

First order system:

$$\ell[u_1] - \ell[\tilde{u}_0] - \frac{1}{r^2}\frac{\partial^2 u_0}{\partial \theta^2} + \frac{dp}{dz} = 0$$

or

$$\frac{\partial^2 u_1}{\partial r^2} + \frac{1}{r}\frac{\partial u_1}{\partial r} - \frac{M^2}{r^2}u_1 + \frac{1}{r^2}\frac{\partial^2 u_0}{\partial \theta^2} - \frac{M^2}{r^2}u_1 = \frac{dp}{dz} \tag{22}$$

$$u_1 = 0, \text{ at } r = r_2$$

$$u_1 = 0, \text{ at } r = r_1 \tag{23}$$

The solution of the above linear ordinary differential equation is given in

$$u_1 = \frac{1}{4M(-4+M^2)}\mathrm{Csch}[M\mathrm{Log}[\frac{r_1}{r_2}]](-4M\frac{\partial p}{\partial z}r^2\mathrm{Sinh}[M(\mathrm{Log}[\frac{r_1}{r_2}])]$$

$$(4r_2^2 M\frac{\partial p}{\partial z} - g(-4+M^2)(\mathrm{Log}[\frac{rr_1}{r_2}])\mathrm{Sinh}[M(\mathrm{Log}[\frac{r_1}{r}])] -$$

$$4r_1^2 M\frac{\partial p}{\partial z}\mathrm{Sinh}[M(\mathrm{Log}[\frac{r_2}{r}])] + g(-4+M^2)$$

$$(\mathrm{Log}[\frac{r_1}{r}])\,\mathrm{Sinh}[M(\mathrm{Log}[\frac{rr_1}{r_2}])]$$

Where

$$g = \frac{1}{r_1^2}M V \varepsilon\,\mathrm{Csch}[M(\mathrm{Log}[\frac{r_1}{r_2}]))]\,r_1\,\mathrm{Coth}[M(\mathrm{Log}[\frac{r_1}{r_2}])] +$$

$$M\varepsilon(1 + 2\,\mathrm{Csch}^2[M(M(\mathrm{Log}[\frac{r_1}{r_2}])\,\mathrm{Sin}^2[\theta]$$

Finally, for $f \to 1$, we approach the final solution. So from Eq. (16), we get

$$\tilde{u}(r,\theta,z,t) = u_0 + u_1 \tag{24}$$

where u_0 and u_1 are defined in Eq. (20).
The instantaneous volume flow rate $\overline{Q}(z,t)$ is given by

$$\overline{Q}(z,t) = 2\pi\int_{r_1}^{r_2} rudr, \tag{25}$$

$$\frac{\overline{Q}}{2\pi} = \frac{1}{4M(-4+M^2)^2}((4+M^2)(2g r_2^2 + (r_1^4 - r_2^4)M\frac{\partial p}{\partial z}) +$$

$$2(r_1^2\mathrm{Cosh}[M(\mathrm{Log}[\frac{r_1}{r_2}])](-g(4+M^2) + 2M(g\ \mathrm{Coth}\ [M(\mathrm{Log}[\frac{r_1}{r_2}])]$$

$$(-2(r_1^4 + r_2^4)M\frac{\partial p}{\partial z} + g r_2^2(-4+M^2)(\mathrm{Log}[\frac{r_1}{r_2}]) + M(-4+M^2)$$

$$V\mathrm{Csch}[M((\mathrm{Log}[\frac{r_2}{r_1}]))](-2(r_1^4 + r_2^4)M\frac{\partial p}{\partial z} + g r_2^2(-4+M^2)(\mathrm{Log}[\frac{r_1}{r_2}])$$

$$+ r_1^2\mathrm{Csch}[M(\mathrm{Log}[\frac{r_1}{r_2}])](-2g + 4r_2^2 M\frac{\partial p}{\partial z} + g(-4+M^2)((\mathrm{Log}[\frac{r_2}{r_1}])$$

$$+ 2g r_1^2\ \mathrm{Sinh}[M(\mathrm{Log}[\frac{r_1}{r_2}])] - 2(-4+M^2)V\mathrm{Csch}[M(\mathrm{Log}[\frac{r_2}{r_1}])]$$

$$(r_2^2 M + 2r_1^2\ \mathrm{Sinh}[M(\mathrm{Log}[\frac{r_1}{r_2}])))) \tag{26}$$

The mean volume flow rate Q over one period is given as [7]

$$\overline{Q}(z,t) = \frac{Q}{\pi} - \frac{\phi^{*2}}{2} + \xi\, z\, \phi\, \mathbf{Cos}[2\pi(z-t)] + 2\phi^* \cos[2\pi(z-t)] + \phi^{*2}\cos^2[2\pi(z-t)] \tag{27}$$

Now pressure gradient $\frac{\partial p}{\partial z}$ will be evaluated by using Eqs. (26) and (27)

$$\frac{dp}{dz} = (2M(-4+M^2)^2(\overline{Q} - \frac{1}{M(-4+M^2)}\pi(g r_2^2(4+M^2) r_1^2\ \mathrm{Cosh}[M(\mathrm{Log}[\frac{r_1}{r_2}]$$

$$(-g(4+M^2) + 2M^2(-4+M^2)V\,\mathrm{Csch}[M(\mathrm{Log}[\frac{r_2}{r_1}])] + g r_1^2 M\,\mathrm{Csch}[M(\mathrm{Log}[\frac{r_1}{r_2}])]$$

$$(-2 + 2\,\mathrm{Cosh}[2M(\mathrm{Log}[\frac{r_1}{r_2}] - (-4+M^2)\mathrm{Log}[r_1] + (-4+M^2)\mathrm{Log}[r_2]) + (-4M + M^3)$$

$$(g r_2^2\mathrm{Coth}[M(\mathrm{Log}[\frac{r_1}{r_2}])]((\mathrm{Log}[\frac{r_1}{r_2}])) - 2V\mathrm{Csch}[M(\mathrm{Log}[\frac{r_2}{r_1}])](M r_2^2$$

$$+ 2r_1^2\mathrm{Sinh}[M(\mathrm{Log}[\frac{r_1}{r_2}])])))) / \pi((2g r_2^2 + ((r_1^4 - r_2^4)M)(4+M^2) - 2g r_1^2(4+M^2)$$

$$\mathrm{Cosh}[M(\mathrm{Log}[\frac{r_1}{r_2}] + 2M\mathrm{Coth}[M(\mathrm{Log}[\frac{r_1}{r_2}](-2M(r_1^4 - r_2^4) + g r_2^2(-4+M^2)(\mathrm{Log}[\frac{r_1}{r_2}])$$

$$+ 2r_1^2 M\mathrm{Csch}[M(\mathrm{Log}[\frac{r_1}{r_2}])](-2g + 4r_2^2 M + 2g\mathrm{Cosh}[2M(\mathrm{Log}[\frac{r_1}{r_2}] + g(-4+M^2)$$

$$((\mathrm{Log}[\frac{r_2}{r_1}])) \tag{28}$$

The pressure rise $\Delta p(t)$ in non-dimensional form is defined as

$$\Delta p(t) = \int_0^1 \frac{\partial p}{\partial z}dz \tag{29}$$

4 Results And Discussion

The analytical and numerical results obtained above for the given analysis are discussed graphically The graphical treatment for the data of pressure rise Δp, pressure gradient and velocity profile u(r, θ, z, t) with the variation of all emerging dimensionless parameters like time t, flow rate Q, the taper parameter ζ, the velocity of the inner tube V, the eccentricity parameter ε and the MHD parameter M has been analyzed. In the end, the stream lines observing the peristaltic flow are drawn for the parameters M, Q and ζ while other parameters remain fixed. The comparison graph for the values obtained in present work with the results of R. Ellahi et. al. [8] is displayed in figures. The graphs for the pressure rise Δp(t) versus flow rate Q under the effects of given parameters are drawn in figs 2-6. These graphs show the pumping regions, that is, the peristaltic (Q > 0,Δ p > 0), the augmented pumping (Q > 0,Δ p < 0) and the retrograde pumping (Q < 0,Δ p > 0) The pressure gradient against the the coordinate Z with the variation of pertinent parameters are shown in figs 7-10. The velocity field u(r,θ, z, t) versus the radial coordinate r is plotted in fig.s 11-15 for both two and

three dimensions. The streamline graphs are shown in figs. 16 -18 fig 2 is plotted to see the variation of pressure rise for different values of the eccentricity parameter ε and the angle θ while all other parameters are kept fixed. It is observed that peristaltic pumping region is in between Q ∈ [0, 0.7], augmented pumping is in Q ∈ [0.7, 2] and retrograde pumping part is Q ∈ [−1, 0]. It is also observed from this graph that the pressure rise increases with the variation of ε but decreases with the angle θ in between the region Q ∈ [−1, 0.7] and opposite behavior is seen in the remaining part. The graph of pressure rise for the parameter M and δ is plotted in fig 3. Fig 4. Shows that the peristaltic pumping part is Q ∈[0, 0.3] when varies values of ε and ϕ^* , while augmented and retrograde pumping regions are Q∈ [0.3, 2] and Q ∈ [−1, 0], respectively. We note that the pressure rise in fig 5. Increase whenever the taper parameter ζ into smaller values, The variation of pressure rise Δp in V is similar to that of M (See fig 6). The pressure gradient for the parameters M and δ is drawn in fig 7. It is measured from this figure that pressure gradient is in linear relation to both of the parameters in the narrowest parts of the cylinders but inverse relation is seen in the wider parts. The variation of pressure gradient with the parameters ζ and ε is very much similar to that of the parameters M and δ and is shown in fig 8. The only difference is that the pressure gradient is minimum on the left and right sides of the cylinder while appears maximum at the centre. It means that flow can easily pass without imposition of large pressure gradient in the two sides of the channel while much pressure gradient is required to maintain the flux in the central part near z = 0.8. This is in good agreement with the physical condition. Also, for a diverging tapering with angle ζ. Figs (8.a) extending case ζ > 0 figs (8.b), the pressure gradient values higher than all other existing results corresponding to converging tapering case ζ <0 .It can be observed from figs 9 and 10 that the pressure gradient increases with the parameters Q and V, while when δ is increased the pressure gradient decreases on the left and right sides but increases at the centre of the cylinders. It is also seen that the variation of pressure gradient remains same in the two sides of the cylinders and become different at the central part with changing V but this variation remains same throughout for the parameter Q. The fig 11 shows that the velocity field is an increasing function of the parameter δ while decreasing with the parameter M. The velocity field is in inverse relation with Q but have a direct variation with ε (see fig 12). It is also observed that the presence of a magnetic field for fluid causes to slow down the flow. It is observed from fig 13 that the velocity distribution is increasing with δ and ϕ^* while reducing for t. Fig 14 shows that the velocity profile is linearly changing with ϕ^* and V. The Fig 15 shows that velocity in the case ζ > 0 at (15.a) higher than reported in the case ζ ≤ 0 at (15.b). Fig 16 is drown to see the streamlines for the parameter M. It is measured from this figure that numbers of bolus are not changing but size is increasing with the increasing effects of M at the bottom of the cylinder, while bolus are lessened in number when seen in the upper part. The boluses are reduced both in size and number when seen in the parameter Q in both parts of the geometry (see fig 17). Fig 16 is drawn to see the streamlines for the parameter M..It is measured from this figure that numbers of bolus are not changing but size is decreasing with the increasing effects of M in the upper part of the cylinder, while bolus are disappears when seen in the bottom part. The boluses are reduced both in size and number when seen for the parameter Q in both parts of the geometry (see fig 17). It is seen from fig 18 that the numbers of bolus are decreasing With different values of the parameter ζ on both sides of the cylinder but in the lower half of the tube, the bolus becomes smaller with increasing magnitude of the parameter ζ >0 also the Incompressible fluid from the left side. On the contrary, the bolus fade out with less values of ζ <0 and the Incompressible fluid from the right side

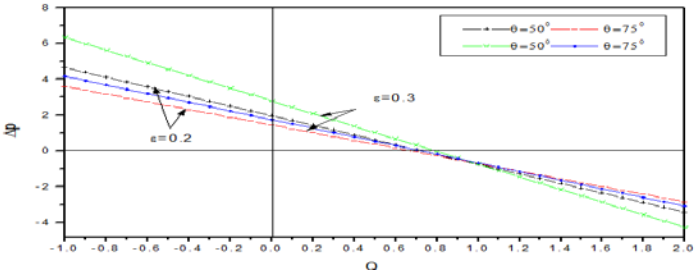

Fig 2 Pressure *rise* versus flow rate for fixed parameters

$\phi^* = 0.2, \zeta = 0, t = 0.1, \delta = 0.1, M = 0.5, V = 0.5$

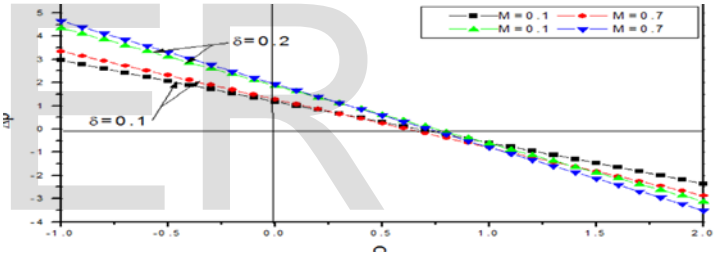

Fig 3 *Pressure rise versus flow rate for fixed parameters*

$\phi^* = 0.2, \zeta = 0, t = 0.1, \varepsilon = 0.01, \theta = 50^0, V = 0.5$

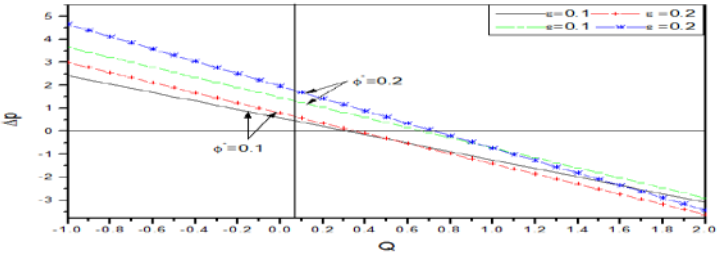

Fig 4 Pressure rise versus flow rate for fixed parameters

$\theta = 50^0, \zeta = 0, t = 0.1, \delta = 0.1, M = 0.5, V = 0.5$

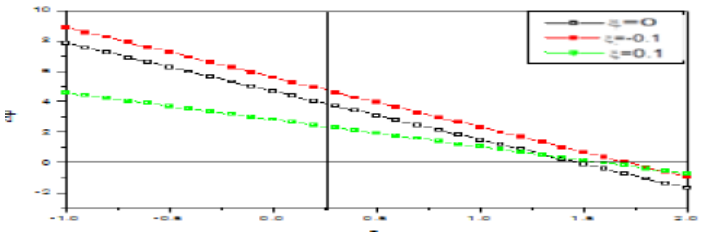

Fig 5 Pressure rise versus flow rate for fixed parameters

$\theta = 50^0, \varepsilon = 0.01, t = 0.1, \delta = 0.1, M = 0.5, V = 0.5$

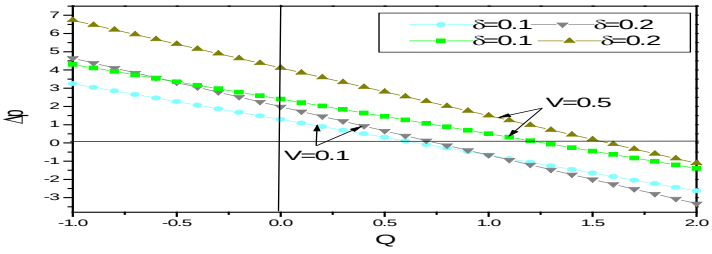

Fig 6 Pressure rise versus flow rate for fixed parameters $\phi^* = 0.2, \zeta = 0, t = 0.1, \varepsilon = 0.01, M = 0.5, \theta = 50^0$

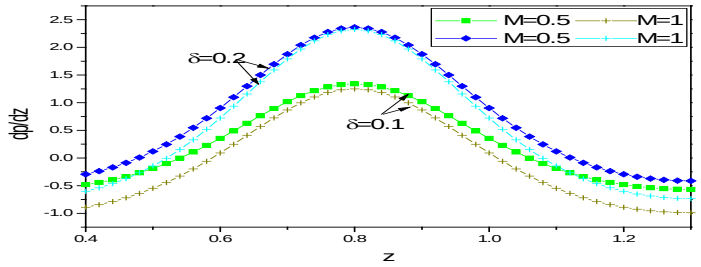

Fig 7 *Variation of pressure gradient with z for fixed parameters* $\phi^* = 0.1, \zeta = 0, t = 0.3, \theta = 50^0, \varepsilon = 0.01, V = 0.3, Q = 0.5$

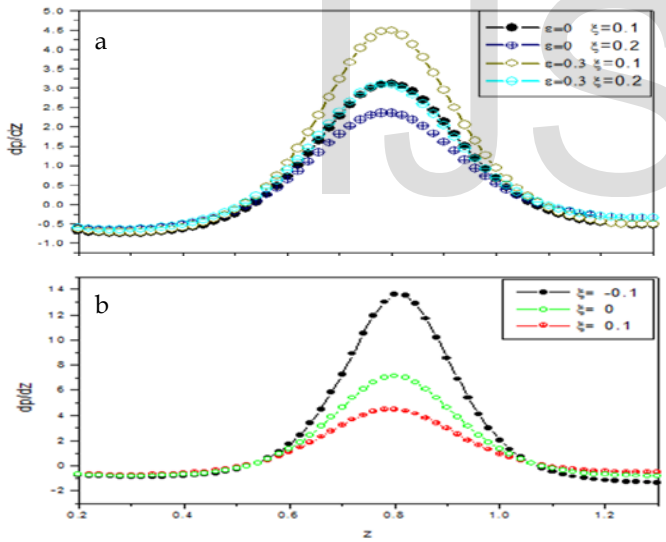

Fig 8 *Variation of pressure gradient with z for fixed parameters* $M = 0.5, t = 0.3, \theta = 50^0, \varepsilon = 0.01, V = 0.3, Q = 0.5$

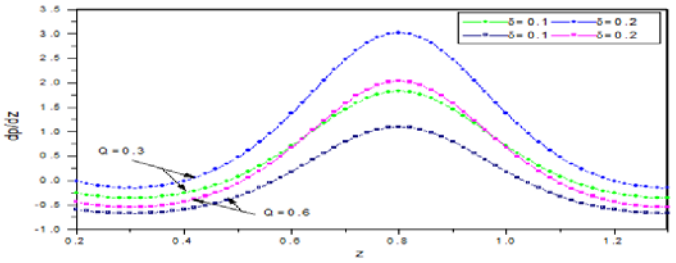

Fig 9 Variation of pressure gradient with z for fixed *Parameters* $M = 0.5, t = 0.3, \theta = 50^0, \varepsilon = 0.01, V = 0.3, Q = 0.5$

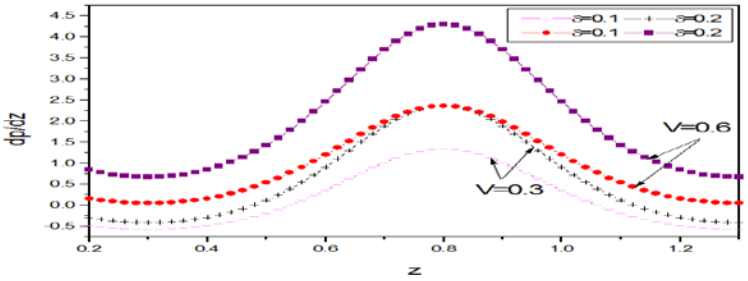

Fig 10 Variation of pressure gradient with z for fixed param ters $\phi^* = 0.1, \zeta = 0, t = 0.3, \theta = 50^0, \varepsilon = 0.01, M = 0.5, V = 0.3$

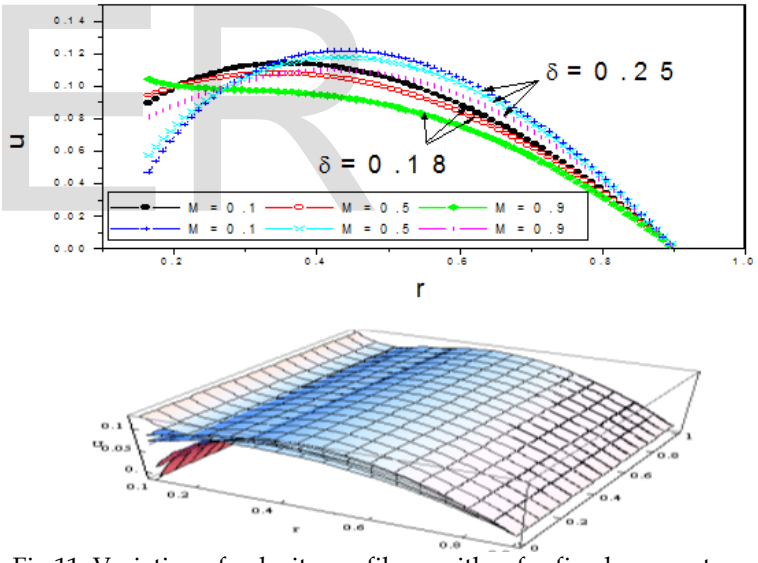

Fig 11 Variation of velocity profile u with r for fixed parameters

$z = 0, \phi = 0.1, \zeta = 0, \theta = 75^{\circ}, V = 0.1, Q = 0.5, t = 0.5, \varepsilon = 0.1$

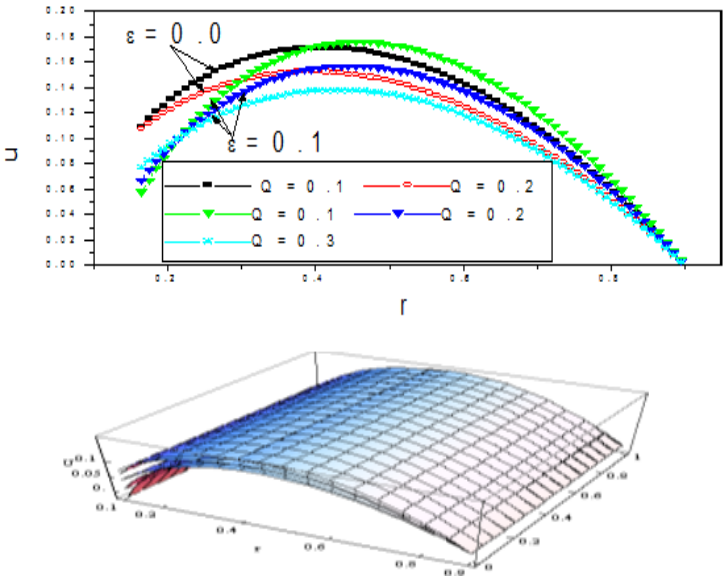

Fig 12 Variation of velocity profile u with r for fixed parameters
$z = 0, \phi^{*} = 0.1, \zeta = 0, \theta = 75^{0}, V = 0.1, Q = 0.5, t = 0.5, \varepsilon = 0.1$

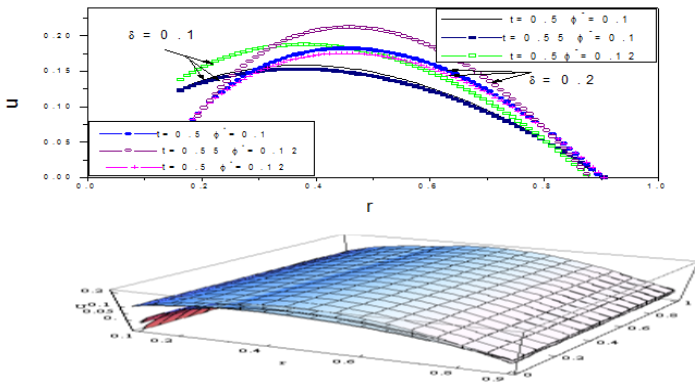

Fig 13 Variation of velocity profile u with r for fixed parameters $z=0, \phi^{*}=0.1, \zeta=0, \theta=75^{0}, V=0.1, Q=0.1, \varepsilon=0.01, M=0.5$

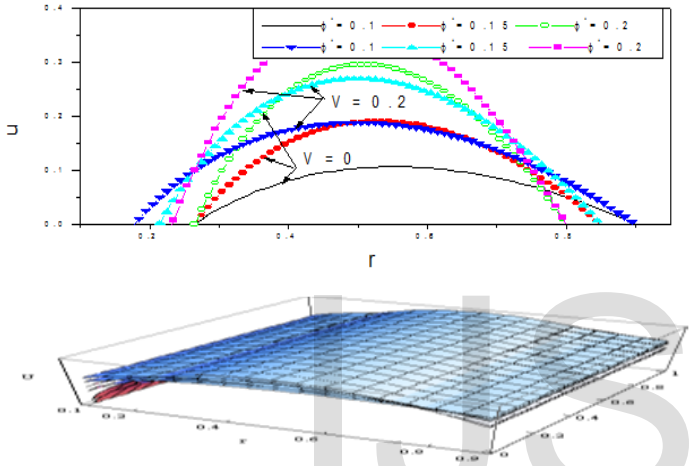

Fig14 Variation of velocity profile u with r for fixed parameters $z=0, \zeta=0, \theta=50^{0}, Q=0.1, t=0.5, \delta=0.2, \varepsilon=0.1, M=0.5$

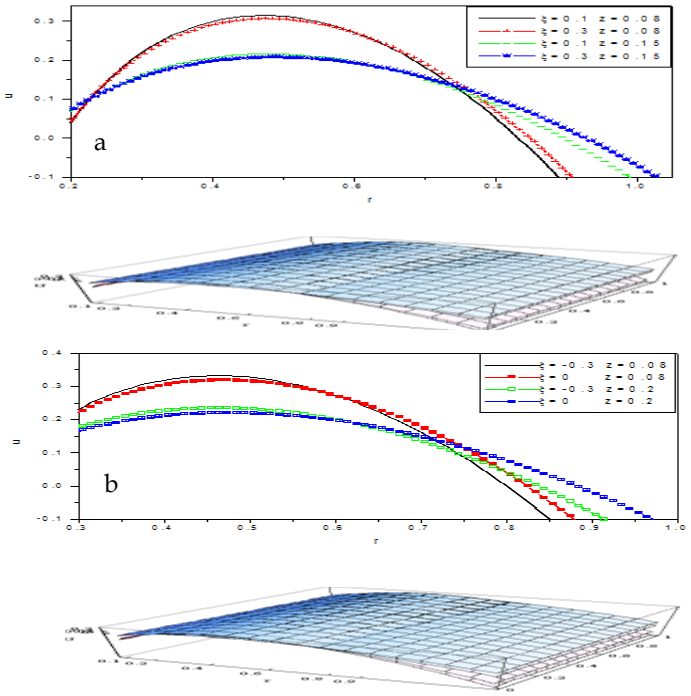

Fig 15 Variation of velocity profile u with r for fixed parameters $\theta=50^{0}, \phi^{*}=0.2, Q=0.1, t=0.5, \delta=0.2, \varepsilon=0.1, M=0.5$

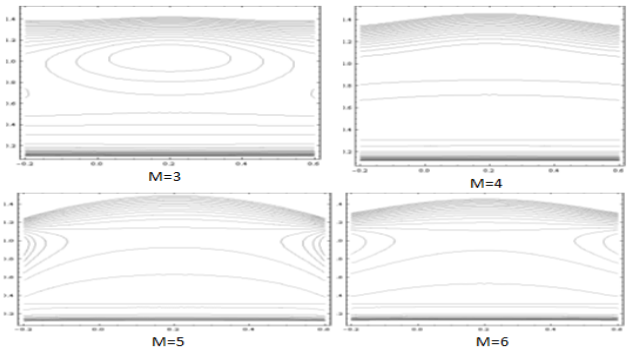

Fig 16 Streamlines for different values of M for The other parameter are $\theta=50^{0}, \phi^{*}=0.02, V=0.3, Q=1, t=0.2, \delta=0.05, \varepsilon=0.4, \zeta=0$

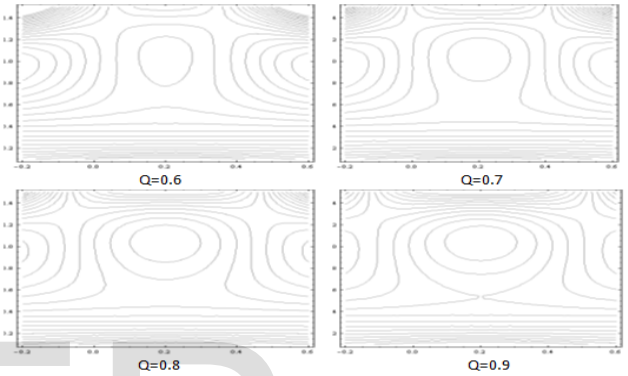

Fig 17 Streamlines for different values of Q for The other parameters are $\theta=50^{0}, \phi^{*}=0.05, V=0.3, M=1, t=0.5, \delta=0.05, \varepsilon=0.4, \zeta=0$

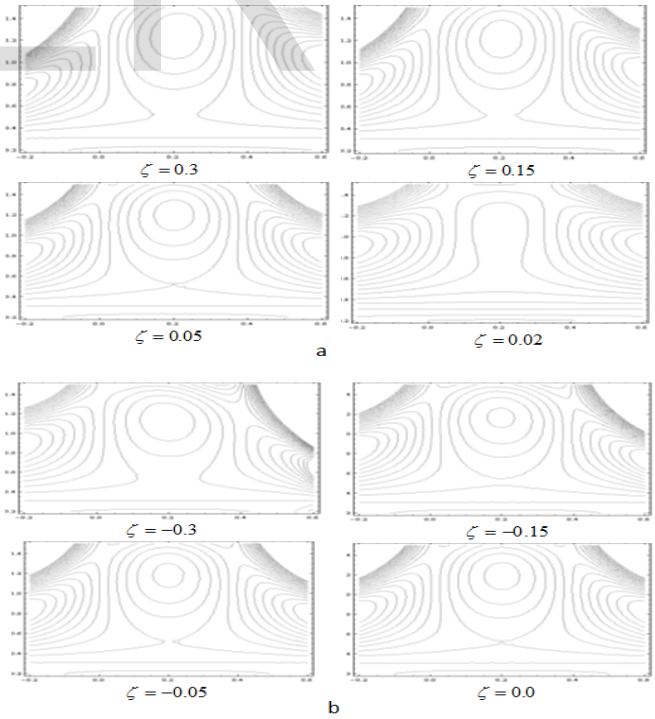

Fig 18 Streamlines for different values of a for (ζ >0), b for (ζ ≤0.0) The of the parameters are $\theta=50^{0}, \phi^{*}=0.2, V=0.3, Q=0.6, t=0.5, \delta=0.05, \varepsilon=0.4, M=0.3$

5 Concluding Remark

In the present investigation Homotopy perturbation method solutions are presented for the peristaltic flow of MHD fluid between two eccentric tubes. The inner tube is rigid and the outer have a sinusoidal wave generated on the walls of tapered. The problem is measuring under the assumptions of long wavelength and low Reynolds number. The following observations have been found:

- It is observed that pressure rise is decreasing function of taper parameter ζ and θ while it increasing function of radius δ, magnetic field M
- Pressure rise is increasing function of eccentricity parameter, amplitude ratio ϕ^* and the velocity of the inner tube V.
- The pressure gradient increases with radius δ, eccentricity parameter ε and the velocity of the inner tube V while decrease with flow rate Q, taper parameter ζ and magnetic field M.
- The velocity profile is increasing with the increase in radius, amplitude ratio ϕ^* and eccentricity parameter ε while decrease with the flow rate Q, magnetic field M and taper parameter,
- The velocity in the case of eccentric cylinders higher than concentric one
- It is depicted that the number of bolus is changing inversely with taper parameter ζ and flow rate Q while not changing increasing effects of magnetic field M but dimensions.

Bibliography

[1] Jaffrin, M.Y., & Shapiro, A.H. (1971). Peristaltic pumping. Annual Review of Fluid Mechanics, 3(1), 13-37.

[2] Shapiro, A.H., Jaffrin, M.Y., & Weinberg, S.L. (1969). Peristaltic pumping with long wavelengths at low Reynolds number. Journal of Fluid Mechanics, 37(04), 799-825.

[3] Colgan, T., & Terrill, R.M. (1987). On peristaltic transport of fluids. Journal de mécanique théorique et appliquée, 6 (1), 3-22.

[4] Barton, C., & Raynor, S. (1968). Peristaltic flow in tubes. The Bulletin of mathematical biophysics, 30 (4), 663-680.

[5] Rachid, H., & Ouazzani, M.T. (2008). The Effect of a Pulsatile flow on the peristaltic output: Case of a Newtonian Fluid. Adv. Studies Theor. Phys., 2 (6), 291-307

[6] Afifi, N.A.S., & Gad, N.S. (2003). Interaction of peristaltic flow with pulsatile fluid through a porous medium. Applied mathematics and computation, 142 (1), 167-176..

[7] Mekheimer, K.S. (2008). Effect of the induced magnetic field on peristaltic flow of a couple stress fluid. Physics Letters A, 372 (23), 4271-4278.

[8] Ellahi, R., Riaz, A., Nadeem, S., & Mushtaq, M. (2013). Series solutions of magnetohydrodynamic peristaltic flow of a Jeffrey fluid in eccentric cylinders. Appl. Math, 7(4), 1441-1449.

[9] Kothandapani, M., & Srinivas, S. (2008). Peristaltic transport of a Jeffrey fluid under the effect of magnetic field in an asymmetric channel. International Journal of Non-Linear Mechanics, 43 (9), 915-924.

[10] Hayat, T., Javed, M., & Asghar, S. (2008). MHD peristaltic motion of Johnson–Segalman fluid in a channel with compliant walls. Physics Letters A, 372(30), 5026-5036.

[11] Nadeem, S., & Akbar, N. S. (2012). Endoscopic and heat transfer effects on the peristaltic flow of a third-order fluid with chemical reactions. Asia-Pacific Journal of Chemical Engineering, 7(1), 45-54.